



Cone Beam CT with Automatic vessel Detection Software versus Conventional 2D Fluoroscopy with Overlay for Prostate Artery Embolization: A Comparison of Prostatic Artery Catheterization Time and Radiation Exposure

Vedant Acharya¹ Hamed Jalaieian² Srinivas Tummala² Kush Shah³ Jessica Kumar³ Issam Kably² Shivank Bhatia²

¹ University of Miami Miller School of Medicine, Miami, Florida, United States

² Department of Interventional Radiology, University of Miami Miller School of Medicine, Miami, Florida, United States

³ Department of Interventional Radiology, Jackson Memorial Hospital, Miami, Florida, United States

Address for correspondence Vedant Acharya, BS, Department of Interventional Radiology, University of Miami - Miller School of Medicine, 1150 NW 14th ST, Suite 702, Miami, FL 33136-2118, United States (e-mail: v.acharya1@med.miami.edu).

J Clin Interv Radiol ISVIR 2022;6:90–97.

Abstract

Purpose To evaluate the effect of cone-beam computed tomography (CT) with automatic vessel detection software on prostate artery catheterization and fluoroscopy time in prostate artery embolization (PAE).

Methods Fifty patients undergoing PAE for BPH were enrolled in this prospective study. Twenty-five PAEs were performed using automatic vessel detection software with syngo embolization guidance (study) and were compared with 25 PAEs performed using conventional two-dimensional (2D) fluoroscopy with overlay (control). PAE was performed using 300–500 μm trisacryl gelatin spherical particles. The primary outcome parameters were prostatic artery catheterization time and fluoroscopy time.

Results Bilateral PAE was achieved in 24/25 cases in both groups. The median right and left prostatic artery catheterization times were similar between the two groups, ($p=0.473$ and $p=0.659$, respectively). The median fluoroscopy time (28.0 and 42.0 minutes, $p=0.046$) and total procedure time (70.0 and 118.0 minutes, $p<0.001$) were shorter in the study group. The median total dose area product (DAP) was not significantly different. However, the median CBCT DAP (11406 vs. 6248, $p<0.001$) was higher in the study group, while median fluoroscopy DAP (7371 vs. 8426, $p<.049$) was higher in the control group. Median digital subtraction angiography (DSA), CBCT, and fluoroscopy DAP accounted for 27%, 45%, and 29% of the total

Keywords

- ▶ prostate artery embolization
- ▶ automatic vessel detection software
- ▶ cone-beam computed tomography

published online
July 2, 2022

DOI <https://doi.org/10.1055/s-0041-1740575>.
ISSN 2457-0214.

© 2022. Indian Society of Vascular and Interventional Radiology. All rights reserved.

This is an open access article published by Thieme under the terms of the Creative Commons Attribution-NonDerivative-NonCommercial-License, permitting copying and reproduction so long as the original work is given appropriate credit. Contents may not be used for commercial purposes, or adapted, remixed, transformed or built upon. (<https://creativecommons.org/licenses/by-nc-nd/4.0/>)

Thieme Medical and Scientific Publishers Pvt. Ltd., A-12, 2nd Floor, Sector 2, Noida-201301 UP, India

DAP in the study group and 32%, 29%, and 39% in the control group ($p < 0.001$), respectively. All complications were Clavien–Dindo Grade 1.

Conclusion Although CBCT with automatic vessel detection software had no significant effect on time-to-prostatic artery catheterization and total radiation exposure, it reduced the fluoroscopy time and procedure time.

Introduction

Prostate artery embolization (PAE) requires precise identification and characterization of the prostatic arteries to ensure technical and clinical success with minimal complications. Identification of prostatic arteries can be very challenging; prostatic arteries have significant variability in origin, diameter, tortuosity, and number.^{1,2} Proper identification and characterization of the prostatic arteries influence the catheter and guidewire selection and impact the radiation dose, procedure time, and safety of the procedure.^{1,3} Cone Beam computed tomography (CBCT) is utilized in combination with direct contrast injection and two-dimensional (2D) fluoroscopy roadmap overlays to help alleviate some of these challenges.^{4,5} However, routine use may be limited by the time necessary to review the volumetric datasets to accurately depict the prostatic artery and potential extraprostatic supply.⁴ To reduce these limitations, companies have developed three-dimensional (3D) CBCT vessel detection software to automatically detect and reconstruct the 3D virtual arterial supply.

Evidence regarding the efficacy of CBCT with automatic vessel detection software in reducing prostate artery embolization catheterization time and radiation exposure is limited. Chiradia et al evaluated six patients in a single-arm study and found that the vessel detection software had a 92% sensitivity in identifying prostate arteries and the mean fluoroscopy time was 47 minutes.⁶ Schott et al evaluated 100 patients in a single-arm retrospective study and found that the use of vessel detection software resulted in an average procedure time and fluoroscopy time of 89.4 minutes and 30.9 minutes, respectively.⁷ This prospective double-arm study was performed to assess the clinical application of CBCT with automatic vessel detection software (syngo Embolization Guidance, Siemens Healthineers, Siemens Medical Solutions, Malvern, PA) compared with 2D fluoroscopy with overlay in PAE. The primary objective of this study was to evaluate the use of CBCT with automatic vessel detection software on prostate artery catheterization time and radiation exposure as measured by fluoroscopy time.

Materials and Methods

This single-center, prospective study was approved by the local institution institutional review board (IRB) (ClinicalTrials.gov Identifier: NCT03164629). During routine consultation for PAE, patients were offered participation in the

study; if they were willing to participate, informed consent was obtained. Inclusion criteria were patients aged 50 to 79 years of age, with LUTS or urinary retention secondary to BPH without any contraindications to PAE (ex: coagulopathy, urinary tract infection, or poor renal function). Exclusion criteria included weight greater than 300 pounds and biopsy-proven prostate cancer.

In a nonequivalent control group posttest-only design from June 20, 2017, to July 31, 2018, 50 patients were enrolled prospectively and underwent prostate artery embolization. There was no randomization. The first 25 patients were assigned to the study group and underwent PAE using CBCT with embolization guidance software navigation. For this group, a 3D rotational selective angiography of the internal iliac artery was obtained using a 5 Fr catheter placed in the internal iliac artery with 25 cc of Visipaque (non-diluted) injected for 10 seconds (2.5 cc/sec). After a 5-second X-ray delay, a 6-second spin was performed. A 3D reconstruction was performed on an independent workstation, and a path (Emboguide) was created and displayed on the 2D roadmap. The subsequent set of 25 patients were assigned to the control group and underwent PAE with conventional 2D fluoroscopy with roadmap fluoroscopy overlay. A single interventional radiologist (SB) with ~13 years of experience performed all procedures.

The primary outcome parameters were time-to-prostatic artery catheterization and fluoroscopy time. For the study group, catheterization time was measured from the time that automatic vessel detection software was utilized, and virtual 3D images were reconstructed and displayed over 2D live fluoroscopy images, to the time of prostatic artery catheterization (► Fig. 1). For the control group, catheterization time was measured as the time from when the first digital subtraction angiography (DSA) roadmap images were obtained and overlaid over 2D live fluoroscopy to the time of prostatic artery catheterization.

All procedures were performed in an interventional radiology suite, under local anesthesia with moderate intraprocedural sedation using a Siemens Artis Q ceiling angiography system (Siemens Medical Solutions, Malvern, PA) with either iopamidol (Isovue, Bracco Diagnostics) or iodixanol (Visipaque, GE Healthcare, Marlborough, MA) contrast media. Access was achieved via the left radial artery in 24/25 (96%) of the study group and 25/25 (100%) of the control group. The right femoral artery access was utilized in one patient in the study group. Patients received pre-procedural antibiotics as per institutional guidelines. Automatic vessel detection was performed using the Syngo

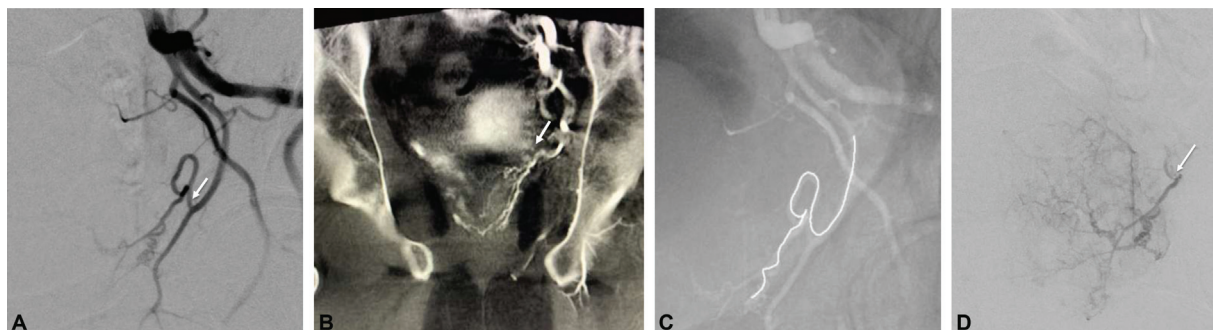


Fig. 1 A 77-year-old man with BPH and LUTS for over 10 years, was initially treated medically with dutasteride. However medical management was discontinued due to medication side effects. The patient underwent PAE using CBCT with embolization guidance software navigation (A–D). (A) Diagnostic angiography of the left internal iliac artery demonstrating the left prostatic artery (arrow) apparently arising from the inferior vesical artery. (B) Coronal reconstruction cone beam CT demonstrating the origin of the left prostatic artery (arrow) arising from the inferior vesical artery. (C) Automatic vessel detection using Syngo Embolization Guidance software reconstructing left prostatic artery virtual image for overlay with 2D live fluoroscopy. (D) Successful catheterization and selective angiography of the left prostatic artery (arrow).

Embolization Guidance software (Siemens Healthineers) installed on a Syngo X workplace (Siemens Healthineers).

Catheterization of the prostatic arteries was performed with a 2.1 Fr Maestro microcatheter (Merit Medical Inc, South Jordan, Utah) and a Fathom-16 steerable guidewire (Boston Scientific, Marlborough, Massachusetts). Embolization was performed using 100–300 μm and/or 300–500 μm trisacryl gelatin spherical particles (Embosphere, Merit Medical Systems, South Jordan, Utah) based on the operator preference. Embolization was performed to stasis while monitoring for reflux.

Additional parameters including dose for planning dataset for each side in the study group, number of DSAs and CBCTs, radiation exposure as measured by dose area product (DAP), prostatic artery tortuosity and origin, total procedure time, technical success, clinical success, and procedure-related complications were also evaluated. Pre and post-PAE prostate volumes were measured by magnetic resonance imaging (MRI) or ultrasound. Technical success was defined as bilateral prostate embolization. Complications were recorded according to the Clavien–Dindo classification.

Statistical Analysis

Shapiro–Wilks test indicated nonparametric distributions for all variables, which are expressed as medians (interquartile range). Categorical variables are expressed as the number of patients (percentage of category). Comparisons between the procedure groups were performed using the Mann–Whitney U test given the nonparametric distributions of the variables, Chi-square (χ^2) test, or Fisher’s exact test, as appropriate. A sample size of 20 patients in each group was estimated using the following parameters: a standard deviation for fluoroscopy time of 18.7 minutes, a type I error of 0.05, a power of 80%, and a difference in fluoroscopy time of 15 minutes. A p -value < 0.05 were considered statistically significant. The analyses were performed using the SPSS software, version 25 (SPSS, Chicago, IL) and RStudio Desktop 1.2.5033 Package (RStudio, Boston, MA).

Results

All enrolled patients in both groups underwent prostate artery embolization. Basic characteristics of the men in the study and control group are listed in **Table 1**; there were no significant differences in baseline characteristics. Both prostatic arteries were identified in all patients. One patient in the control group had a left prostatic artery originating from the right internal iliac artery. Technical success, defined as bilateral prostatic artery embolization, was achieved in 24/25 of patients (96%) in both the study and control groups. Unilateral embolization occurred in both cases of technical failure due to the inability to catheterize the right prostatic artery.

The median right prostatic artery catheterization time was 120.0 seconds (interquartile range [IQR]: 225.0) and 87.5 seconds (IQR: 178.0) in the study and control groups, respectively, ($p = 0.473$). The median left prostatic artery catheterization time was 117.0 seconds (IQR: 220.0) and 135.0 seconds (IQR: 179.3) in the study and control groups, respectively, ($p = 0.659$). The median fluoroscopy time (28.0 vs. 42.0 minutes, $p = 0.046$) and total procedure time (70.0 vs. 118.0 minutes, $p < 0.001$) were significantly shorter in the study group (**Table 2**).

On further evaluation of radiation dose parameters, it was noted that median total DAP was similar between the study and control groups (28498 vs. 27052 $\mu\text{Gy}\cdot\text{m}^2$, $p = 0.484$). However, median CBCT DAP (11406 vs. 6248 $\mu\text{Gy}\cdot\text{m}^2$, $p < 0.001$) was higher and median CBCT number (2 vs. 1, $p = 0.002$) was increased in the study group, while median fluoroscopy DAP (7371 vs. 8426 $\mu\text{Gy}\cdot\text{m}^2$, $p < 0.049$) was increased in the control group. Both groups had a similar median DSA number per patient with similar DSA DAP. The median DSA, CBCT, and fluoroscopy DAP accounted for 27%, 45%, and 29% of the total DAP in the study group and 32%, 29%, and 39% in the control group ($p < 0.001$), respectively (**Table 3**).

All complications in both groups were Clavien–Dindo Grade 1. There were no major complications (**Table 4**).

Table 1 Baseline characteristics and anatomic features of prostatic arteries

	Study Group	Control Group	p-Value
Age, mean, SD	65.3 (SD 7.0)	66.4 (SD 7.1)	0.591
Comorbidities, frequency, %			
Diabetes Mellitus	0 (0%)	1 (4%)	1.00
Hypertension	5 (20%)	6 (24%)	
Hyperlipidemia	3 (12%)	2 (8%)	
Hypertension, Hyperlipidemia	6 (24%)	6 (24%)	
Diabetes, hypertension, Hyperlipidemia	1 (4%)	1 (4%)	
None	10 (40%)	9 (36%)	
Smoking Status, frequency, %			
Never smoked	15 (60%)	14 (56%)	1.00
Former smokers	8 (32%)	9 (36%)	
Current smokers	2 (8%)	2 (8%)	
Presenting complaint, frequency, %			
LUTS	20 (80%)	25 (100%)	0.050
Acute retention of urine	5 (20%)	0 (0%)	
IPSS score, mean, SD	21.6 (7.6)	21.8 (7.1)	0.896
IPSS-QOL, mean, SD	4.2 (1.4)	4.2 (1.4)	0.922
Prostate Size, median, IQR	100.0 (50.0)	96.5 (56.5)	0.884
Initial treatment regiment frequency, %			
No medications	5 (20%)	3 (12%)	0.562
Alpha-blockers only	8 (32%)	7 (28%)	
ARIs only	1 (4%)	3 (12%)	
PDE-5 inhibitors only	0 (0%)	1 (4%)	
Both α blockers and 5ARIs	8 (32%)	5 (20%)	
Other	3 (12%)	6 (24%)	
History of prior surgery frequency, %			
None	20 (80%)	20 (80%)	0.622
TURP	4 (16%)	2 (8%)	
Laser treatment	1 (4%)	1 (4%)	
Other*	0 (0%)	2 (8%)	
Vascular Access, frequency, %			
Radial	24 (96%)	25 (100%)	1.000
Femoral	1 (4%)	0 (0%)	
Prostatic artery origins frequency, %			
Internal iliac	4 (8%)	3 (6%)	0.332
Inferior vesical	16 (32%)	16 (32%)	
Obturator	9 (18%)	4 (8%)	
Internal pudendal	20 (40%)	22 (44%)	
Other less common variants	1 (2%)	5 (10%)	
Left prostate artery tortuosity frequency, %			
Mild	2 (8%)	3 (12%)	1.000
Moderate	20 (80%)	19 (76%)	
Severe	3 (12%)	3 (12%)	

(Continued)

Table 1 (Continued)

	Study Group	Control Group	p-Value
Right prostate artery tortuosity frequency, %			
Mild	0 (0%)	2 (8%)	0.667
Moderate	22 (88%)	21 (84%)	
Severe	3 (12%)	2 (8%)	

*Other procedures include: Transurethral microwave therapy (TUMT) and combination therapy with multiple TURPs and greenlight laser therapy.

Table 2 Comparison of procedural and clinical parameters

	Study group (n = 25)	Control group (n = 25)	p-Value
Technical success frequency, %	24 (96%)	24 (96%)	0.490
Time to catheterization (R) (sec) median, IQR	120.0 (225.0)	87.5 (178.00)	0.473
Time to catheterization (L) (sec) median, IQR	117.0 (220.0)	135.0 (179.3)	0.659
Contrast volume (mL) median, IQR	125 (45)	110 (51)	0.992
Total procedure time (min) median, IQR	70.0 (27.5)	118.0 (43.5)	0.000*
IPSS at 3 months median, IQR	6.0 (6.0)	8.5 (11.5)	0.203
QOL at 3 months Mean, SD	1.0 (1.5)	2.5 (3.8)	0.164

*Statistically significant.

Table 3 Comparison of radiation parameters

	Study group (n = 25)	Control group (n = 25)	p-Value
Fluoroscopy time (min) median, IQR	28.0 (17.5)	42.0 (19.5)	0.046*
Skin dose (mGy) median, IQR	805 (844)	1167 (1631)	0.311
3D CBCT planning dataset dose (R) (mGy) average (Std.)	172.0 (21.4)	NA	NA
3D CBCT planning dataset dose (L) (mGy) Average (Std.)	168.8 (20.7)	NA	NA
DSA DAP ($\mu\text{Gy}\cdot\text{m}^2$) Median (IQR)	6797 (6086)	7027 (9517)	0.271
CBCT DAP ($\mu\text{Gy}\cdot\text{m}^2$) Median (IQR)	11406 (6196)	6428 (6706)	0.000*
Fluoroscopy DAP ($\mu\text{Gy}\cdot\text{m}^2$) Median (IQR)	7371 (6630)	8426 (7449)	0.049*
Total dose area product μ ($\text{Gy}\cdot\text{m}^2$) Median (IQR)	28498 (12301)	27052 (20875)	0.484
Total number of DSA Median (IQR)	9 (5)	10 (4)	0.354
Total number of CBCT Median (range)	2 (2–5)	1 (0–4)	0.002*

Abbreviations: CBCT, cone-beam computed tomography; DAP, dose area product; DSA, digital subtraction angiography.

*Statistically significant.

Discussion

The purpose of this study was to evaluate the effect of CBCT with automatic vessel detection software on prostate artery catheterization time and radiation exposure. The use of the vessel detection software did not significantly affect the catheterization time as originally hypothesized. Although there was a potential risk of increased radiation exposure with CBCT, the study and control groups had similar total DAP. The higher CBCT DAP was offset by a lower fluoroscopy DAP in the study group. These findings suggest that the use of

the automatic vessel detection software may lead to decreased fluoroscopy usage and ultimately a reduction in total procedure time. These findings are hypothesized to occur for three reasons. First, the baseline CBCT from the hypogastric artery confirms the number of vessels supplying the prostate and accurately identifies the collateral circulation and need for potential coiling to avoid non-target embolization. Second, automatic vessel detection reduces the number of DSAs required after catheterization and eliminates the need for repeat CBCTs once catheterization is performed. By eliminating the need for repeat CBCTs post-catheterization, the use of

Table 4 Comparison of complications

Frequency of complications	Study group	Control group	p-Value
Major adverse effects	None	None	0.997
Minor adverse effects			
2+ Cases	Dysuria Frequency Hematuria Nocturia Pain (access site, urethral, rectal, pelvic) Urgency	Dysuria Fever Frequency Hematuria Nocturia Pain (access site, urethral, rectal, pelvic) Urgency	
1–2 Cases	Epididymitis Fever Scrotal swelling Urinary tract Infection	Facial flushing Nausea Penile Discoloration Urinary leakage Urinary spasms	

automatic vessel detection reduces the risk of vessel spasm secondary to keeping the catheter in the prostatic artery while waiting for the CBCT to set up. Finally, the use of automatic vessel detection helps confirm the branches that do not supply the prostate, thereby eliminating the need for unnecessary catheterization.

Different imaging techniques result in variable component DAP proportions. In this study, median DSA, CBCT, and fluoroscopy DAP accounted for 27%, 45%, and 29% of the total DAP in the study group, respectively. In contrast, Schott et al found the average DSA, CBCT, and fluoroscopy DAP percentages to be 43.3%, 30.3%, and 26.4%, respectively, when using the vessel detection software.⁷ Comparison of the DAP values to previous studies is difficult as radiation exposure varies significantly due to several factors including patient demographics, configuration, and characteristics of the angiographic system and detector technology, operator preference, and the applied calculation method of DAP, which can result in deviation up to ± 35%.⁸ However, the increased percentage of CBCT DAP in the study group (compared with the control arm) is thought to be due to the routine use of CBCT, as required by the study protocol, in each hemipelvis with the catheter tip in the internal iliac artery and occasionally with repeat CBCT with the microcatheter in the prostatic artery with super-selective contrast injection to confirm the positioning of the microcatheter and opacification of the prostatic parenchyma.

CBCT has been shown to be effective in identifying the origin of the prostatic arteries and important anastomoses between the prostate arteries and adjacent vessels, which helps prevent non-target embolization to the bladder, rectum, or penis.^{4,9} Because of the rotational nature of the acquisition, which spreads the radiation exposure to the skin and viscera over a 180° arch of the body, a single CBCT can yield the same amount of information as multiple DSA acquisitions with less contrast medium and total radiation exposure, ultimately reducing procedure time.^{5,10} Our study found similar findings; CBCT allowed for shorter fluoroscopy and procedure times. Limitations of CBCT images include

susceptibility to noise, scatter, partial volume effects, truncation, beam hardening, ring and motion artifacts.¹¹

In contrast to CBCT, pre-procedure computed tomography angiogram (CTA) of the pelvis with iodinated contrast has the advantage of mapping out the pelvic arterial vasculature prior to the intervention. Because of the less selective imaging technique, pre-procedure CTA has a particular strength of identifying unusual prostatic artery origins from outside the internal iliac artery.¹² Additionally, pre-procedure evaluation of atherosclerotic disease, parent artery tortuosity, and angle of PA origin can affect the choice of access site, catheter/guidewire selection, and intraprocedural fluoroscopy angulation.¹³ Although our study did not include pre-procedure CTA, the additional radiation dose from pre-procedure CTA can be eliminated by doing intra-procedural CBCT from the internal iliac vessels, with the additional benefit of providing real-time 3D road mapping through automatic vessel tracking software, which increases the sensitivity of identifying small prostatic arteries and collateral arterial supply.^{5,6}

As radiation exposure to both patients and operators is important during PAE, identifying imaging techniques, such as CBCT with automatic vessel detection that help reduce radiation exposure without compromising technical outcomes, is an area of active research interest. Schnapauff et al found that the use of CBCT with semi-automatic feeding vessel detection software identified 100% of prostatic arteries, while the use of internal iliac DSA identified 82% of prostatic arteries ($p = 0.047$).¹⁴ Furthermore, Schott et al, with the use of CBCT with a 3D roadmap software, reported one of the lowest published DAP values for bilateral PAE to date with a mean DAP of 134.4 Gy/cm².⁷

This study had certain limitations. The investigators were not blind to the study arms. Additionally, because of logistical concerns and a learning curve associated with the implementation of new vessel detection software and training of the technologists using the new software, the decision was made to perform PAE in all study group patients consecutively without any randomization. However, the study and

control groups were ultimately comparable (→Table 1). Additionally, the similar catheterization times in the study group and control subjects may not be applicable to operators in different settings (private practice as opposed to academic centers) with less experience in prostatic artery identification and catheterization.

The use of automatic vessel navigation resulted in shorter fluoroscopy time and translated into shorter procedure time with similar total radiation exposure. Automatic vessel navigation software in combination with CBCT could be considered as a problem-solving tool to help reduce fluoroscopy and procedural times.

Authors' Contributions

V Acharya: Acquisition/analysis, interpretation of data, drafting, and revision of submitted work.

H Jalaeian: Acquisition/analysis, interpretation of data, drafting, and revision of submitted work.

S Tummala: Acquisition/analysis, interpretation of data, drafting, and revision of submitted work.

K Shah: Acquisition/analysis, interpretation of data, drafting, and revision of submitted work.

J Kumar: Acquisition/analysis, interpretation of data, drafting, and revision of submitted work.

I Kably: Acquisition/analysis, interpretation of data, drafting, and revision of submitted work.

S Bhatia: Conception, design, acquisition, interpretation of data, drafting, revision, and final approval of submitted work.

Compliance with Ethical Standards

1. All procedures performed in studies involving human participants were in accordance with the ethical standards of the institutional and/or national research committee and with the 1964 Helsinki Declaration and its later amendments or comparable ethical standards.
2. Informed consent was obtained from all individual participants involved in the study

Ethical Approval

All procedures performed were in accordance with the ethical standards of the institutional and national research committee and with the 1964 Helsinki declaration and its later amendments or comparable ethical standards. IDE G130237, ClinicalTrials.gov Identifier NCT02173522.

Informed Consent

Informed consent was obtained from all individual participants included in the study.

Consent for Publication

The authors consent to the publisher's sole and exclusive license of the full copyright of the publication.

Statement of Data Access and Integrity

The authors declare that they had full access to all of the data in this study and the author take complete responsi-

bility for the integrity of the data and the accuracy of the data analysis.

Funding

This study was supported in part by a grant from Siemens Healthcare Diagnostics, (Grant/Award Numbers: MIAMI2016ATBHATIC0022371)

Conflict of Interest

Mr. Acharya reports an employment status of non-partner/non-partnership track/employee and reports grants from Siemens Healthcare Diagnostics, during the conduct of the study. Dr. Jalaeian reports an employment status of non-partner/non-partnership track/employee and reports grants from Siemens Healthcare Diagnostics, during the conduct of the study. Dr. Tummala reports an employment status of non-partner/non-partnership track/employee, reports grants from Siemens Healthcare Diagnostics and reports personal fees from Bard Peripheral Vascular Inc., personal fees from Boston Scientific, personal fees from Abbot, outside the submitted work; during the conduct of the study. Dr. Shah reports an employment status of non-partner/non-partnership track/employee and reports grants from Siemens Healthcare Diagnostics, during the conduct of the study. Dr. Kumar reports an employment status of non-partner/non-partnership track/employee and reports grants from Siemens Healthcare Diagnostics, during the conduct of the study. Dr. Kably reports an employment status of non-partner/non-partnership track/employee and reports grants from Siemens Healthcare Diagnostics, during the conduct of the study. Dr. Bhatia reports an employment status of non-partner/non-partnership track/employee and reports grants from Siemens Healthcare Diagnostics, personal fees from Merit Medical Systems, personal fees from Terumo Medical Corporation, personal fees from Mentice, Inc, personal fees from Siemens Medical Solutions, personal fees from Embolix, Inc, outside the submitted work, during the conduct of the study.

References

1. Bilhim T, Pisco JM, Rio Tinto H, et al. Prostatic arterial supply: anatomic and imaging findings relevant for selective arterial embolization. *J Vasc Interv Radiol* 2012;23(11):1403–1415
2. Moya C, Cuesta J, Frieria A, Gil-Vernet Sedó JM, Valderrama-Canales FJ. Cadaveric and radiologic study of the anatomical variations of the prostatic arteries: a review of the literature and a new classification proposal with application to prostatectomy. *Clin Anat* 2017;30(01):71–80
3. de Assis AM, Moreira AM, de Paula Rodrigues VC, et al. Pelvic arterial anatomy relevant to prostatic artery embolisation and proposal for angiographic classification. *Cardiovasc Intervent Radiol* 2015;38(04):855–861
4. Bagla S, Rholl KS, Sterling KM, et al. Utility of cone-beam CT imaging in prostatic artery embolization. *J Vasc Interv Radiol* 2013;24(11):1603–1607
5. Wang MQ, Duan F, Yuan K, Zhang GD, Yan J, Wang Y. Benign prostatic hyperplasia: cone-beam CT in conjunction with DSA for identifying prostatic arterial anatomy. *Radiology* 2017;282(01):271–280
6. Chiaradia M, Radaelli A, Campeggi A, Bouanane M, De La Taille A, Kobeiter H. Automatic three-dimensional detection of prostatic

- arteries using cone-beam CT during prostatic arterial embolization. *J Vasc Interv Radiol* 2015;26(03):413–417
- 7 Schott P, Katoh M, Fischer N, Freyhardt P. Radiation dose in prostatic artery embolization using cone-beam CT and 3D Roadmap software. *J Vasc Interv Radiol* 2019;30(09):1452–1458
 - 8 Lin P-JP, Schueler BA, Balter S, et al. Accuracy and calibration of integrated radiation output indicators in diagnostic radiology: a report of the AAPM Imaging Physics Committee Task Group 190. *Med Phys* 2015;42(12):6815–6829
 - 9 Bhatia S, Sinha V, Bordegaray M, Kably I, Harward S, Narayanan G. Role of coil embolization during prostatic artery embolization: incidence, indications, and safety profile*. *J Vasc Interv Radiol* 2017;28(05):656–664.e3
 - 10 Floridi C, Radaelli A, Abi-Jaoudeh N, et al. C-arm cone-beam computed tomography in interventional oncology: technical aspects and clinical applications. *Radiol Med (Torino)* 2014;119(07):521–532
 - 11 Lechuga L, Weidlich GA. Cone beam CT vs. fan beam CT: a comparison of image quality and dose delivered between two differing CT imaging modalities. *Cureus* 2016;8(09):e778
 - 12 Maclean D, Maher B, Harris M, et al. Planning prostate artery embolisation: is it essential to perform a pre-procedural CTA? *Cardiovasc Intervent Radiol* 2018;41(04):628–632
 - 13 Desai H, Yu H, Ohana E, Gunnell ET, Kim J, Isaacson A. Comparative analysis of cone-beam CT angiogram and conventional CT angiogram for prostatic artery identification prior to embolization. *J Vasc Interv Radiol* 2018;29(02):229–232
 - 14 Schnapauff D, Maxeiner A, Wieners G, et al. Semi-automatic prostatic artery detection using cone-beam CT during prostatic arterial embolization. *Acta Radiol* 2020;61(8):1116–1124